

Calorimetry in Particle Physics

Lecture IV

Hadronic Calorimeters

H. Oberlack
MPI für Physik, Munich

Hadronic Calorimetry: History

Pioneering papers

V. S. Marzin Progr.Elem.Part. and Cosm.Ray
Physics 9 (1967) 245

J. Engler et al. Phys. Lett. 27B (1968) 599

J. Engler, W. Flauger, B. Gibhard, F. Mönnig, K. Runge,
H. Schopper NIM 106 (1973) 189

V. Böhmer et al. NIM 122 (1974) 313

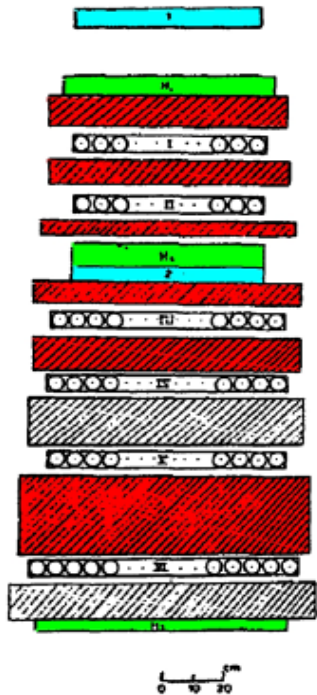
J. Moritz et al. KfK report 1936 (1974)

Cosmic Ray Physics: V. S. Marzin et al.

propose to exploit

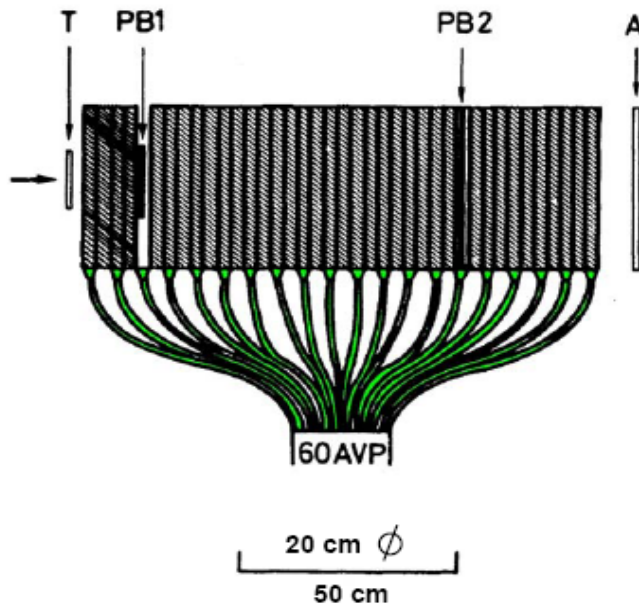
$$\frac{\sigma}{E} \sim \frac{1}{\sqrt{E}}$$

Basic understanding:



- Sampling structure
- $L > 6 \lambda_{abs}$
- converter plates thickness $< 6 X_0$ in order to detect π^0
- **not b** properly considered : transverse leakage

Hadronic Calorimetry: History



n-Calorimeters

H. Schopper et al.

- Transverse dimension of shower λ_{int}
- Systematic study of hadron calorimeters
Questions addressed:
- $S \sim E$
 - $\frac{\sigma}{E} \sim \frac{1}{\sqrt{E}}$
 - Shape of signal for monoenergetic particle

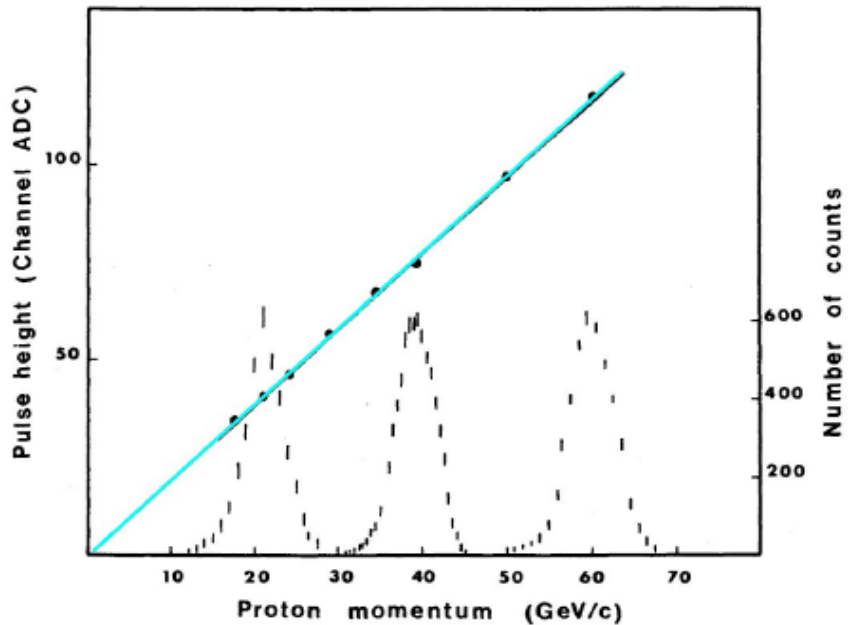
$$n + p \rightarrow p + n$$

inclusive n -spectra

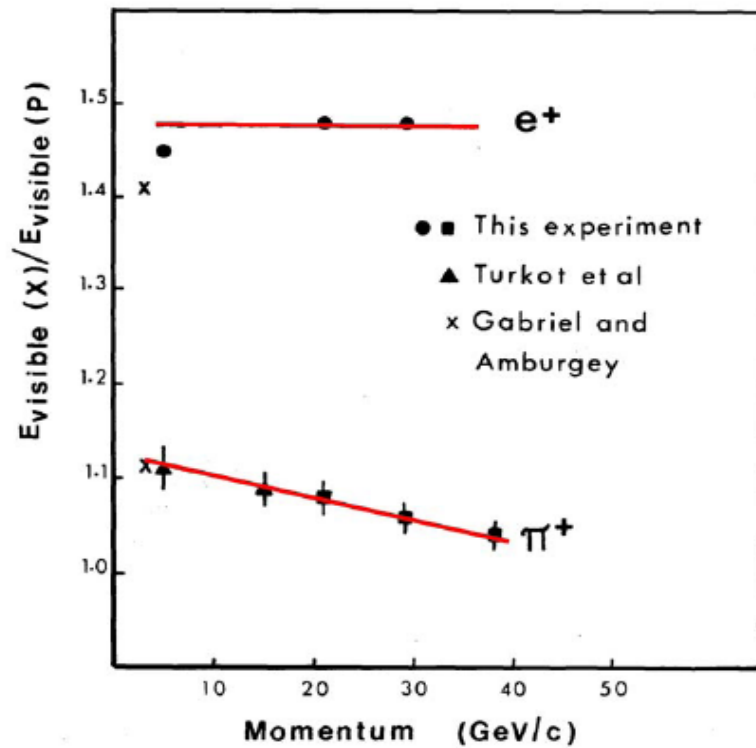
- parameters influencing resolution
- particle identification
- spatial information
- first crude simulation of detector response

Hadronic Calorimetry: History

- Linearity and \sim Gaussian shape



- Different response for e^- and hadrons

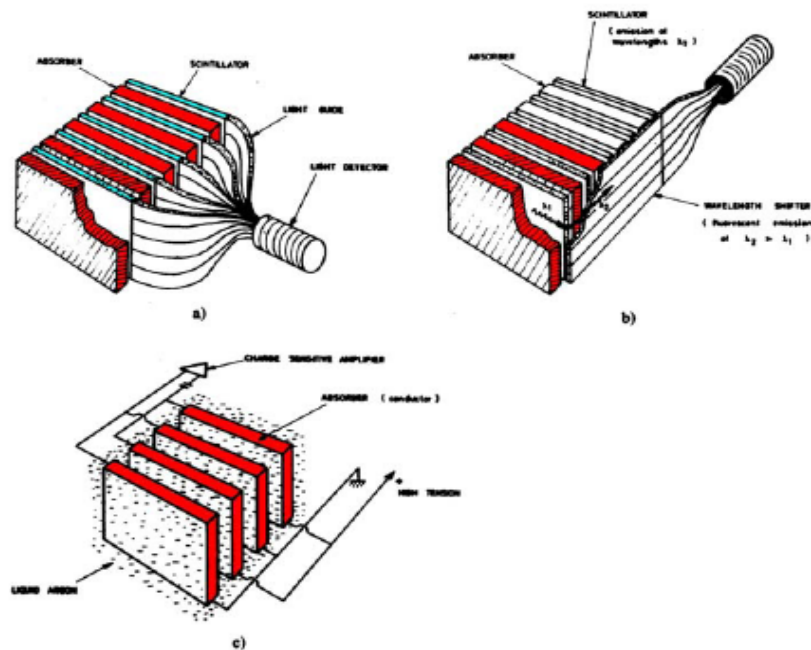


Hadronic Calorimetry: History

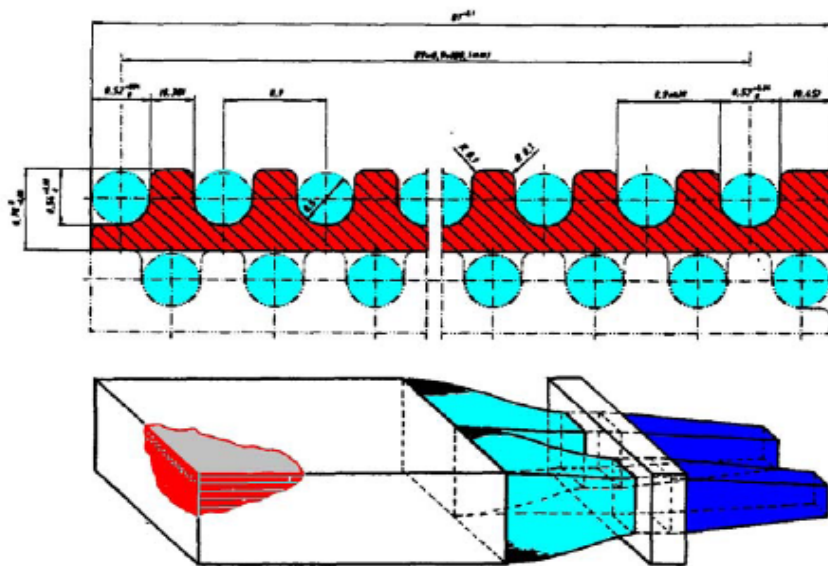
Next step: New read out types

LAr calorimeter: Willis et al.,
Engler et al.

WLS technique: Garwin, Keil,
Hofmann et al.

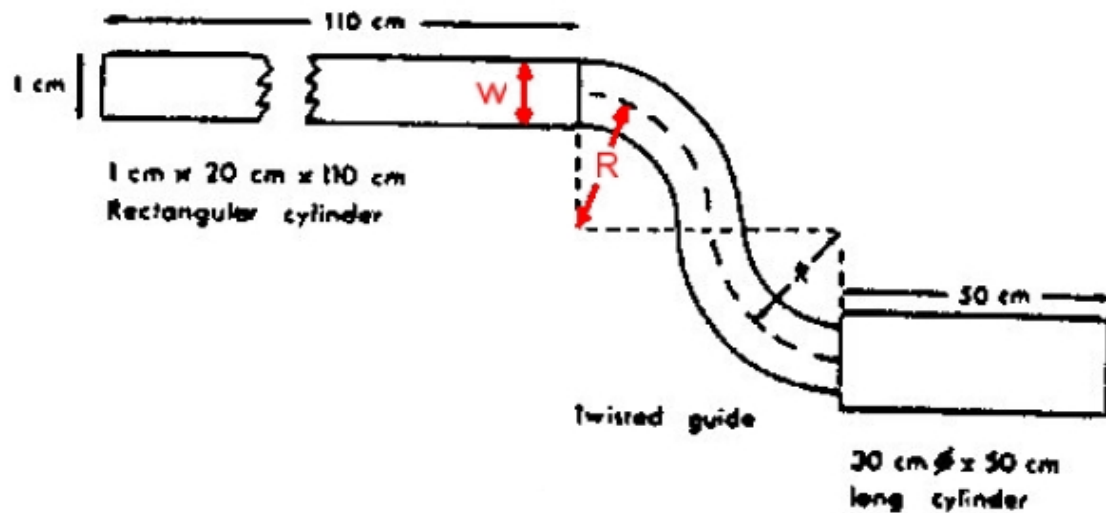


Read-out by scintillating fibres:

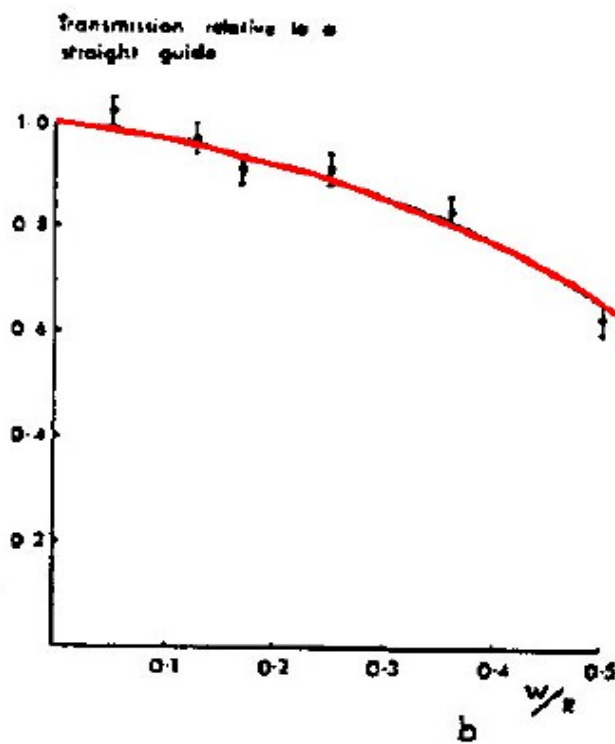


Hadronic Calorimetry: History

Transport of light



Transmission depends on **radius of curvature**

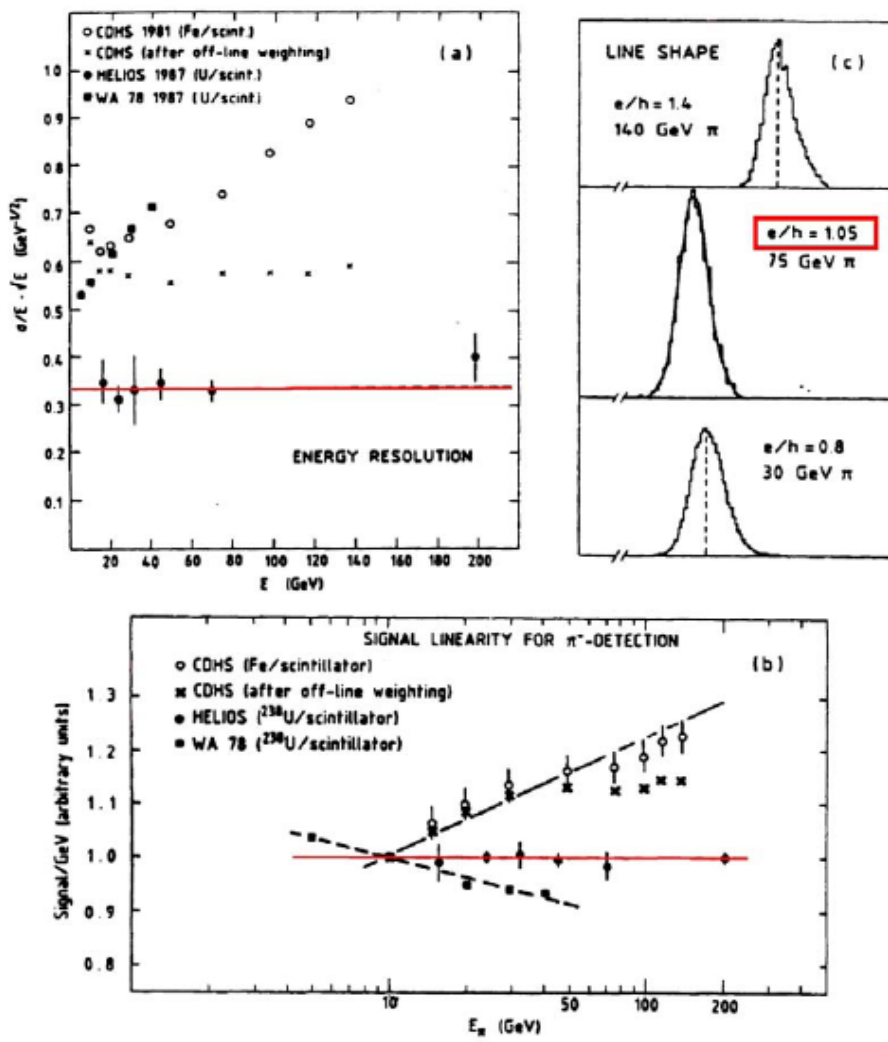


Basic Observations

Aim :

- $S \sim E$
- $\frac{\sigma}{E} \sim \frac{1}{\sqrt{E}}$
- Gaussian shape of signal (unfolding!)
- Signal (e) = Signal (π)

1. Generation of experiments: conditions fulfilled in first approximation, but small deviations:



Basic Observations

These experiments observed

- weak non linearity $\frac{S}{E} \neq const$
- $\frac{\sigma}{E} \cdot \sqrt{E} \neq const$
- non Gaussian tails of signal
- $\frac{S(e)}{S(\pi)} \neq 1$ for $e(\pi)$ of same energy

Detailed studies proved

- Localized energy due to electromagnetic component

$$V_{em} \approx (10X_o \cdot R_M^2) \ll V_{had}(6 \lambda_{int}^3)$$

- $S(e)/S(\pi) \neq 1$ important limitation of energy resolution and linearity

Contributions to Hadron Signal

Energy deposited by a particle i $E_{dep}(i)$

Visible energy $E_V(i)$

Non visible energy (recombination,
nuclear binding) $E_{NV}(i)$

$$a(i) = \frac{E_V(i)}{E_V(i) + E_{NV}(i)} \quad (1)$$

Compare signal with those of min. ionizing particles (**mip**)

High energy μ good approximation to mip

$$\frac{e}{mip} = \frac{a(e)}{a(mip)} \quad (2)$$

Hadronic component of hadronic shower, i.e. electro-magnetic component due to $\pi^0 \rightarrow \gamma\gamma, \omega \rightarrow \pi^0\gamma, \dots$

excluded

$$\frac{h_i}{mip} = \frac{a(h)}{a(mip)} \quad (3)$$

Signal of

$$S(\textcolor{red}{e}) = k \cdot E \cdot \frac{e}{mip} \quad (4)$$

$$S(\textcolor{red}{h}) = k \cdot E \left\{ f_{em} \frac{e}{mip} + (1 - f_{em}) \frac{h_i}{mip} \right\} \quad (5)$$

Calibration constant k : record signal of particles
with well defined energy

$$f_{em} \approx 0.1 \cdot \ln \frac{E}{1 \text{ GeV}} \quad (6)$$

Contributions to Hadron Signal

If

$$\frac{e}{mip} \neq \frac{h_i}{mip} \Leftrightarrow \frac{S(h)}{E} \neq const \quad (7)$$

Discuss ratio

$$\frac{S(e)}{S(h)} = \frac{e/mip}{f_{em} \frac{e}{mip} + (1 - f_{em}) \frac{h_i}{mip}} \quad (8)$$

Conclusions

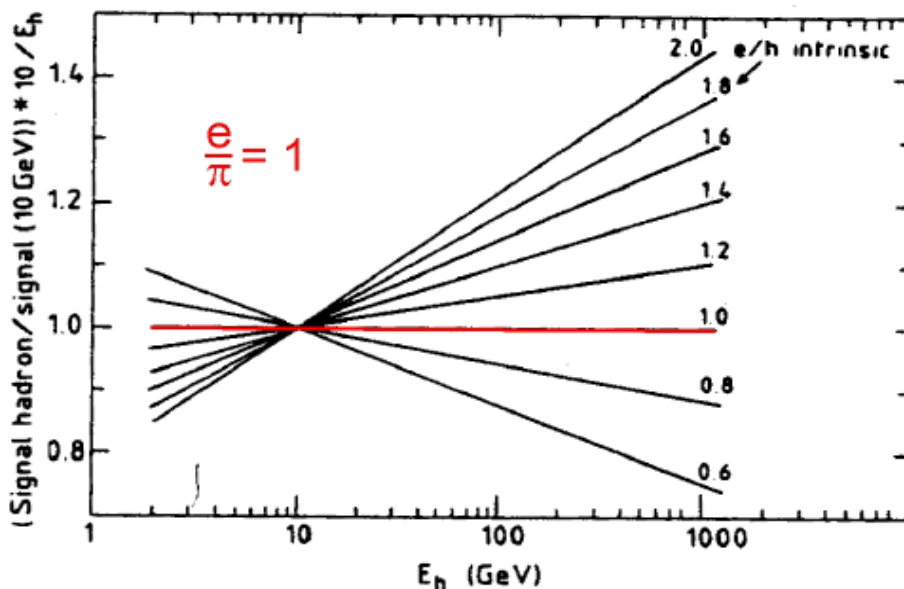
- Since $f_{em} \sim \ln \frac{E}{1GeV}$ energy resolution and signal distribution deteriorate with increasing signal, if

$$\frac{e}{mip} \neq \frac{h_i}{mip}$$

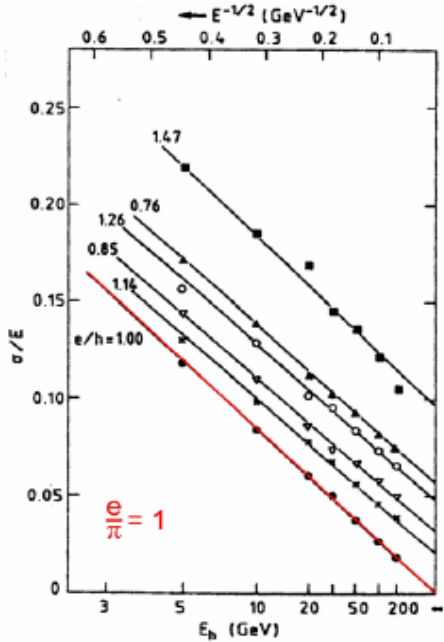
- Deviation from linear dependence

$$S \sim E$$

expected



Contributions to Hadron Signal



Aim of detector lay out

$$\frac{e}{mip} = \frac{h_i}{mip} \quad (9)$$

Different components contribute to $\frac{h_i}{mip}$:

$$\frac{h_i}{mip} = f_{ion} \cdot \frac{ion}{mip} + f_n \cdot \frac{n}{mip} + f_\gamma \cdot \frac{\gamma}{mip} + f_B \cdot \frac{b}{mip}$$

f_{ion} : fraction of hadronic component deposited by charged particles (μ^\pm, π^\mp, p)

f_n : fraction deposited by neutrons (n)

f_γ : fraction deposited by photons (γ) from nuclear deexcitation

f_B : fraction deposited as nuclear binding energy

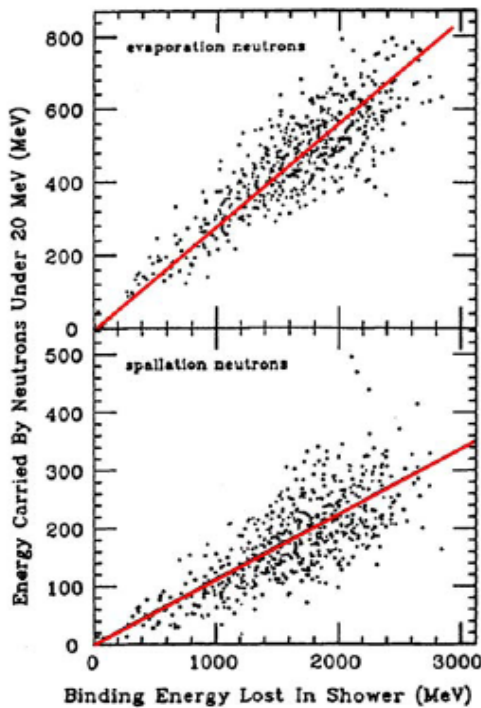
Typical values (Monte Carlo simulation, Wigmans)

Contributions to Hadron Signal

		<i>Fe</i>	<i>U</i>
f_{ion}	total	57 %	38 %
	spallation	42 %	27 %
f_γ		3 %	2 %
f_n		8 %	15 %
f_B		32 %	45 %

	Fe/Sz	Fe/Ar	U/Sz	U/Ar	dependence
$\frac{ion}{mip}$	0.83	0.88	0.91	1	d_{act}
$\frac{n}{mip}$	0.5 ... 2	0	0.8 ... 2.5	0	d_{act}/d_{pas}
$\frac{\gamma}{mip}$	0.7	0.95	0.4	0.4	d_{pas}
$\frac{e}{mip}$	0.9	0.95	0.55	0.55	

Strong correlation of f_B , f_n and f_B , f_γ :



Contributions to Hadron Signal

$$f_B \sim f_n$$

Nuclei excited by n -capture

$$f_\gamma \sim f_n$$

Since for many calorimeters

$$\frac{h_i}{mip} < \frac{e}{mip}$$

\rightsquigarrow increase $\frac{h_i}{mip}$ by

- increase f_n, f_γ
- increase $\frac{n}{mip}, \frac{\gamma}{mip}$
or
- decrease $\frac{e}{mip}$

Applying this condition and achieving

$$\frac{e}{mip} = \frac{h_i}{mip}$$

is the aim of compensation calorimetry

Exploit Monte Carlo Simulation:

Pioneers

H. Brückmann

DESY

R. Wigmans

CERN

Gabriel

Oak Ridge

2 procedures

Software weighting : CDHS, H1

Hardware weighting : Helios, ZEUS

Software Compensation: H1 Method

Highly segmented calorimeter allows to identify regions of high energy deposition (**electromagnetic subshowers**).
Derive from Monte Carlo simulations proper weights

$$\frac{E(Q)}{Q} = \left(A_1 \exp \left\{ -A_2 \frac{Q}{V} \right\} + A_3 \right)_{EMC} + \\ \left(B_1 \exp \left\{ -B_2 \frac{Q}{V} \right\} + B_3 \right)_{HAC}$$

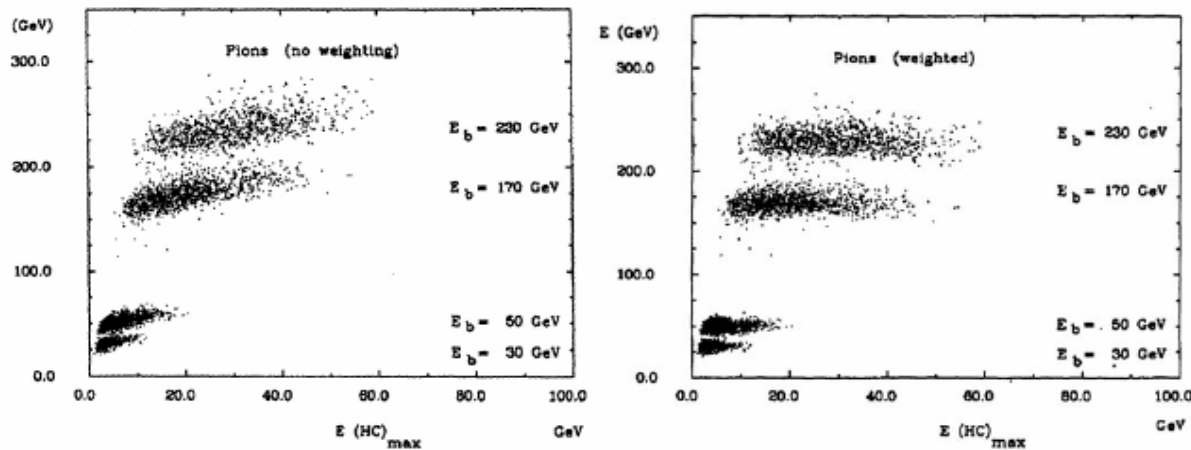
Optimized with MC for different θ, E

Parametrize

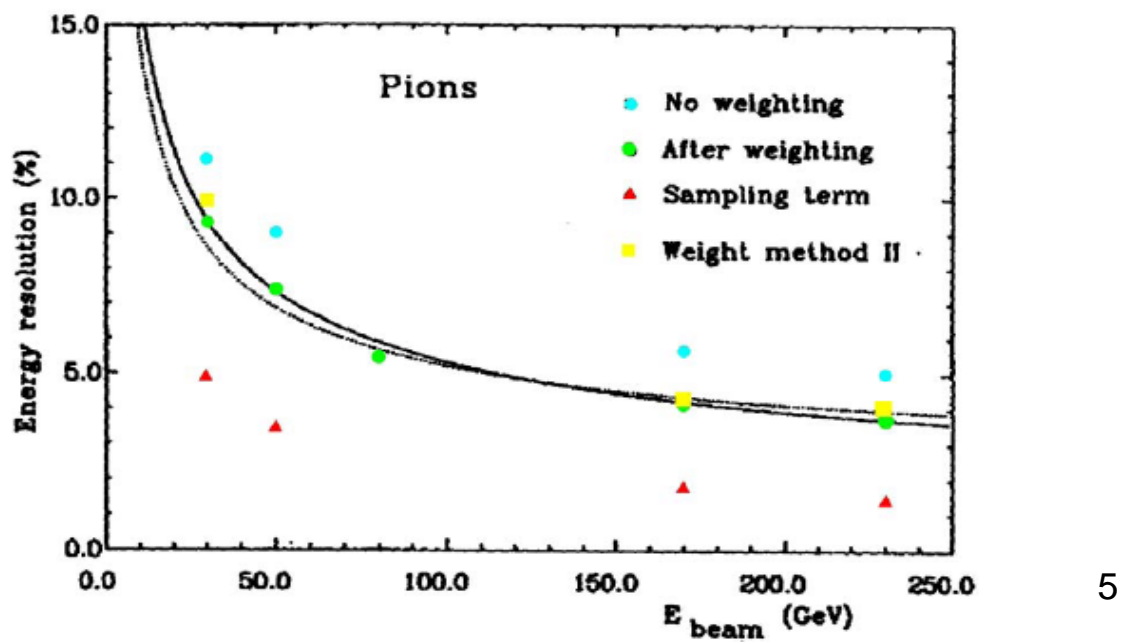
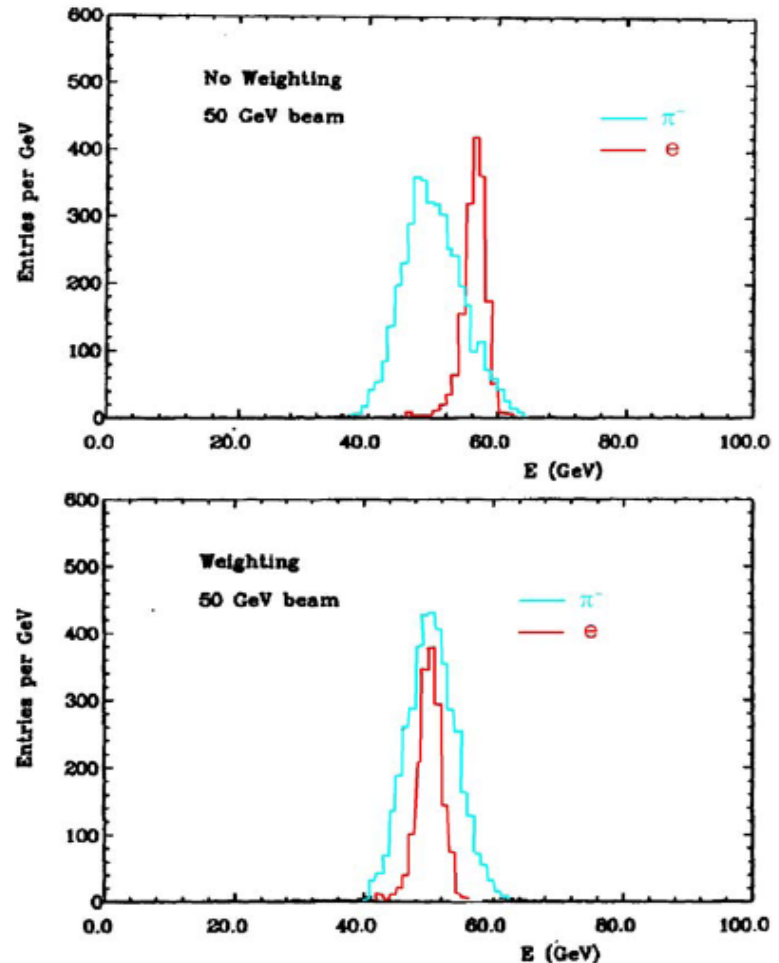
$$A_i = A_i(Q) \quad i = 1, 2$$

$$A_3 = A_3(Q, \theta)$$

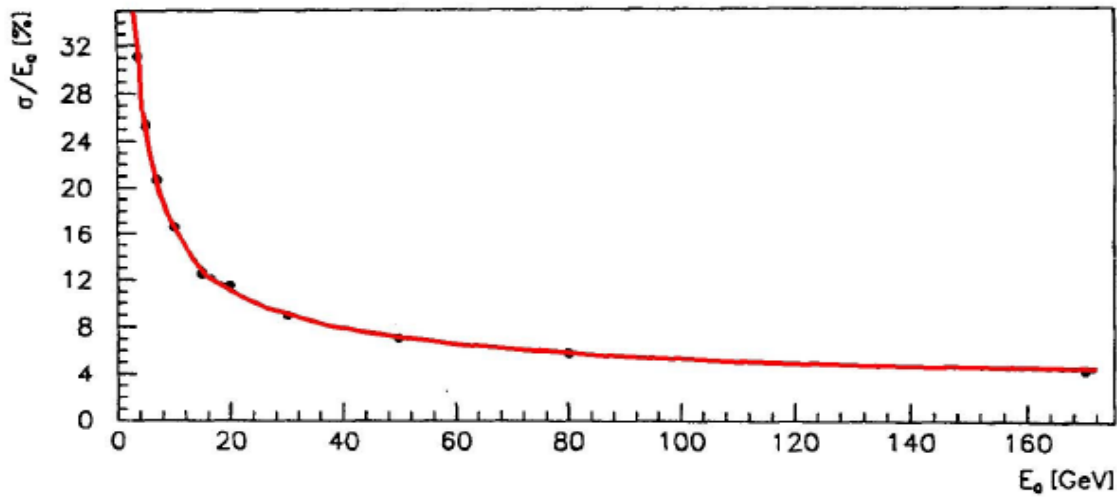
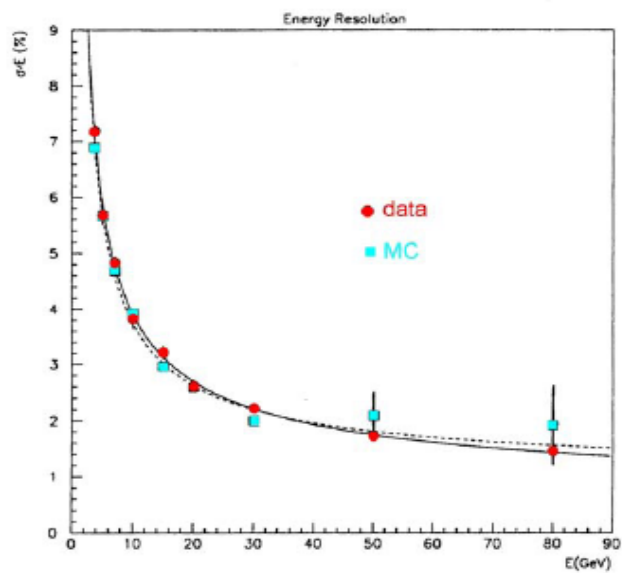
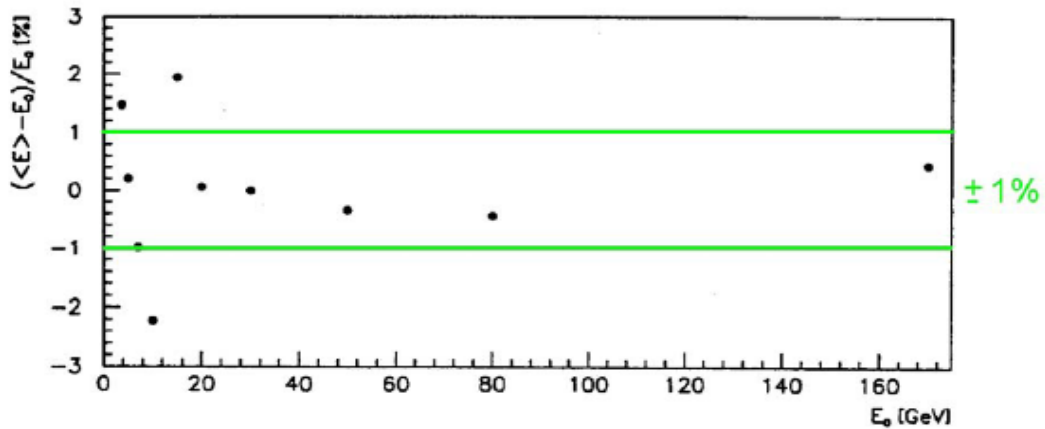
Result:



Software Compensation: H1 Method



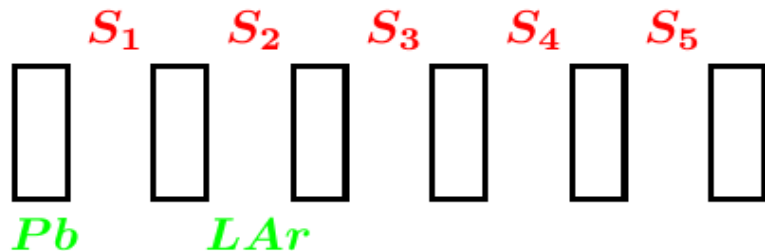
Software Compensation: H1 Method



Software Compensation: H1 Method

- Linearity within 1%
- $S(e)/S(\pi) = 1$
- $\left(\frac{\sigma}{E}\right)_h = \frac{0.46 \text{ GeV}^{1/2}}{\sqrt{E}} \oplus \frac{0.73 \text{ GeV}}{E} \oplus 0.026$

Measurement of sampling fluctuations

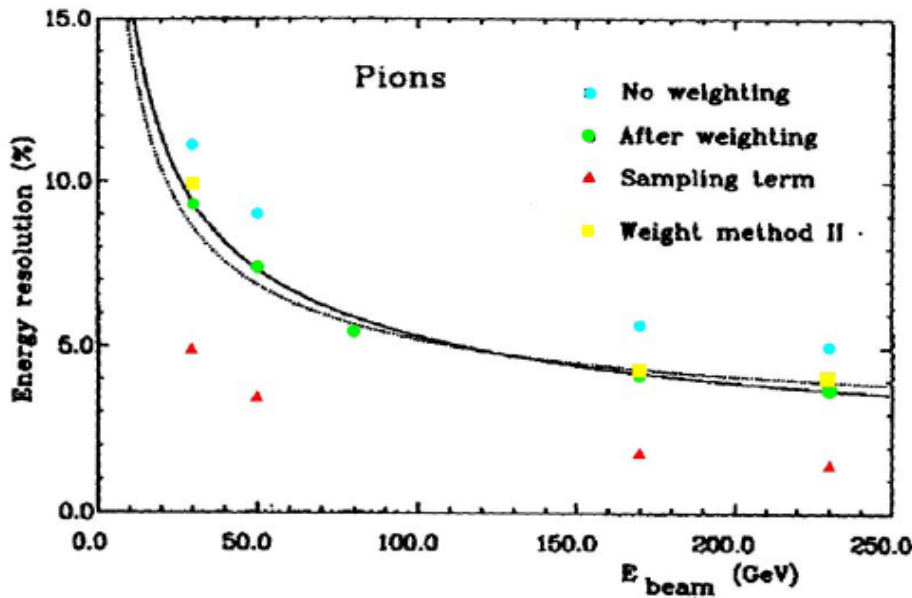


$$S_{\Sigma} = S_1 + S_3 + S_5 + \dots + S_2 + S_4 + S_6 \dots$$

$$S_{\Delta} = S_1 - S_2 + S_3 - S_4 + S_5 - S_6$$

$$\sigma_{\Sigma} = \sigma_{2n} \oplus \sigma_{2n+1} \oplus \sigma_{bind}$$

$$\sigma_{\Delta} = \sigma_{2n} \oplus \sigma_{2n+1}$$

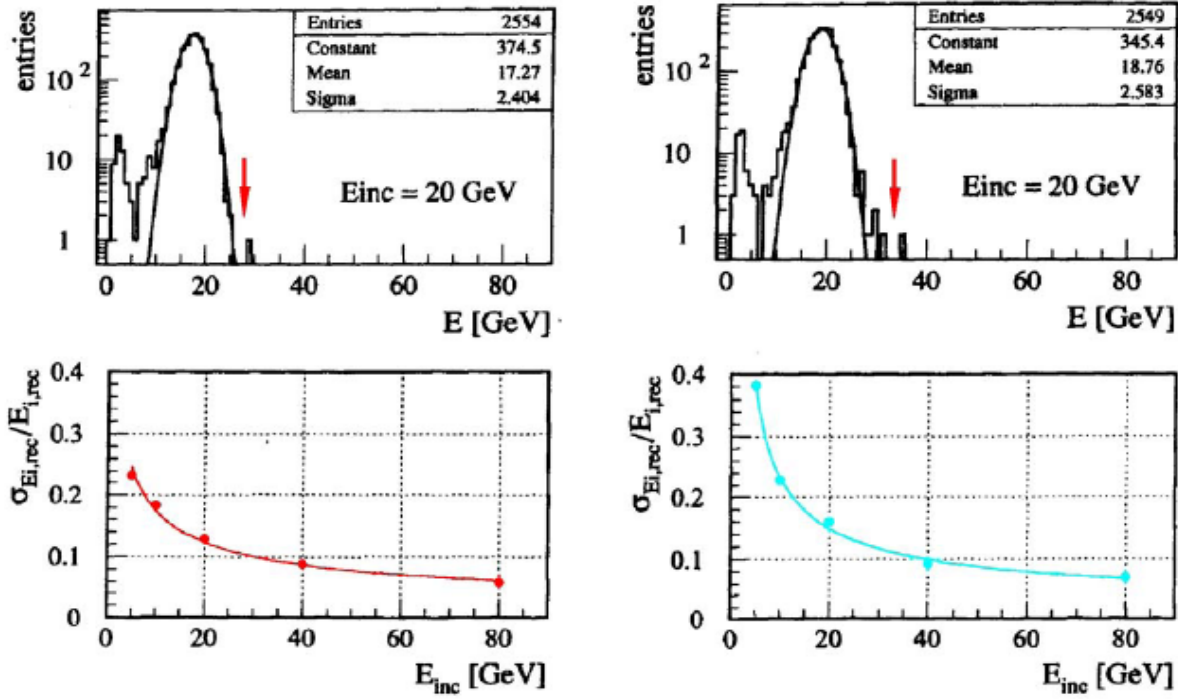


Nuclear binding fluctuations dominate

Software Compensation: H1 Method

Improvements possible

Apply weights via **neural network** tuned with Monte Carlo data :



Got better linearity and resolution for $E < 10 \text{ GeV}$;
for $E > 10 \text{ GeV}$ same results as standard weighting

Hardware Compensation: ZEUS

Aim

$$\frac{e}{mip} = \frac{h_i}{mip}$$

Qualitative discussion of result backed by Monte Carlo simulation (Wigmans, Brückmann)

- $E_n > 1 \text{ GeV}$
 $f_{ion}, f_\gamma, f_n, f_B$ independent of hadron energy
- spallation protons dominant contribution to

$$f_{ion} \rightsquigarrow$$

f_{ion} decreases for increasing $Z (\frac{Z}{A} \searrow)$

- f_n increases, if Z_{abs} increases ($\frac{A-Z}{Z} \nearrow$)
Can only be exploited, if $\frac{n}{mip} \neq 0$
Efficient use only if active material contains H-atoms
This signal is delayed !

Choice of optimal detector material :

$$\frac{h_i}{mip} = \frac{ion}{mip} \cdot f_{ion} + f_n \frac{n}{mip} + f_\gamma \frac{\gamma}{mip} + f_B \frac{b}{mip}$$

Hardware Compensation: ZEUS

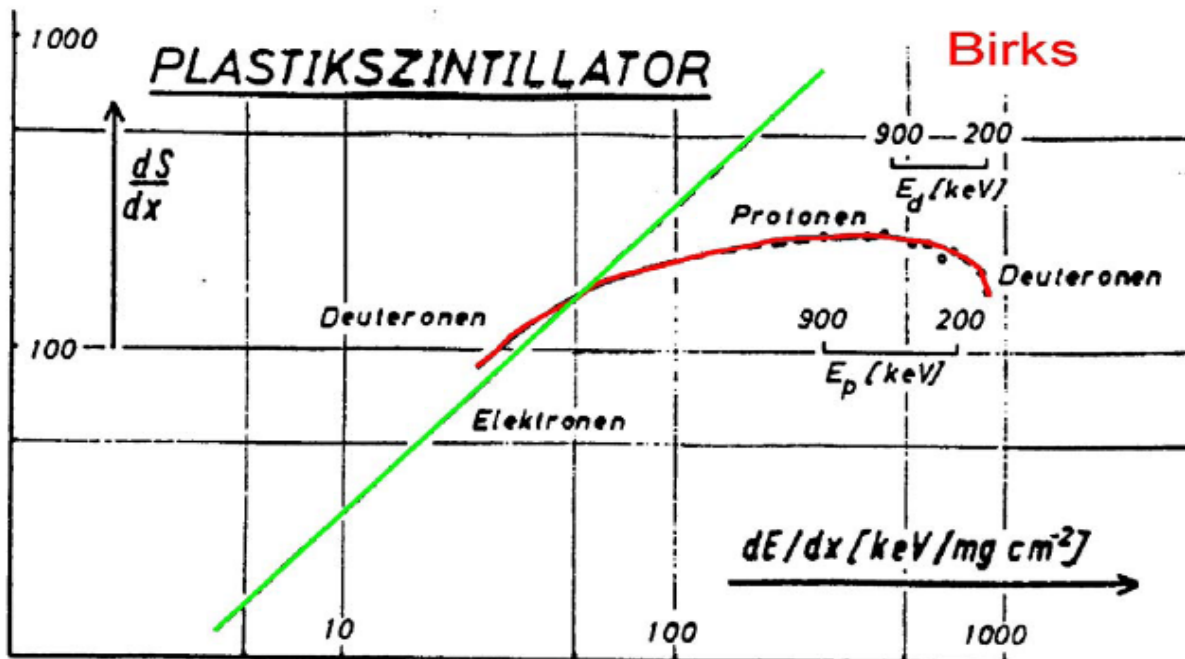
- $\frac{ion}{mip} = 0.8 \dots 1$

Ratio depends on energy spectrum of spallation protons

Ratio depends on $\frac{dE}{dx}$

Birks :

$$\frac{dS}{dx} = \frac{A \frac{dE}{dx}}{1 + k_B \frac{dE}{dx}} = \begin{cases} A \frac{dE}{dx} & E_n \gg m_n \\ A/B & \text{slow particles} \end{cases}$$



Hardware Compensation: ZEUS

$\frac{ion}{mip} \searrow$, if $d_{act} \nearrow$, since $\frac{dE}{dx}$ rises at end of track

If $d_{abs} \ll R_{Spallation}$

\rightsquigarrow all spallation protons enter active medium

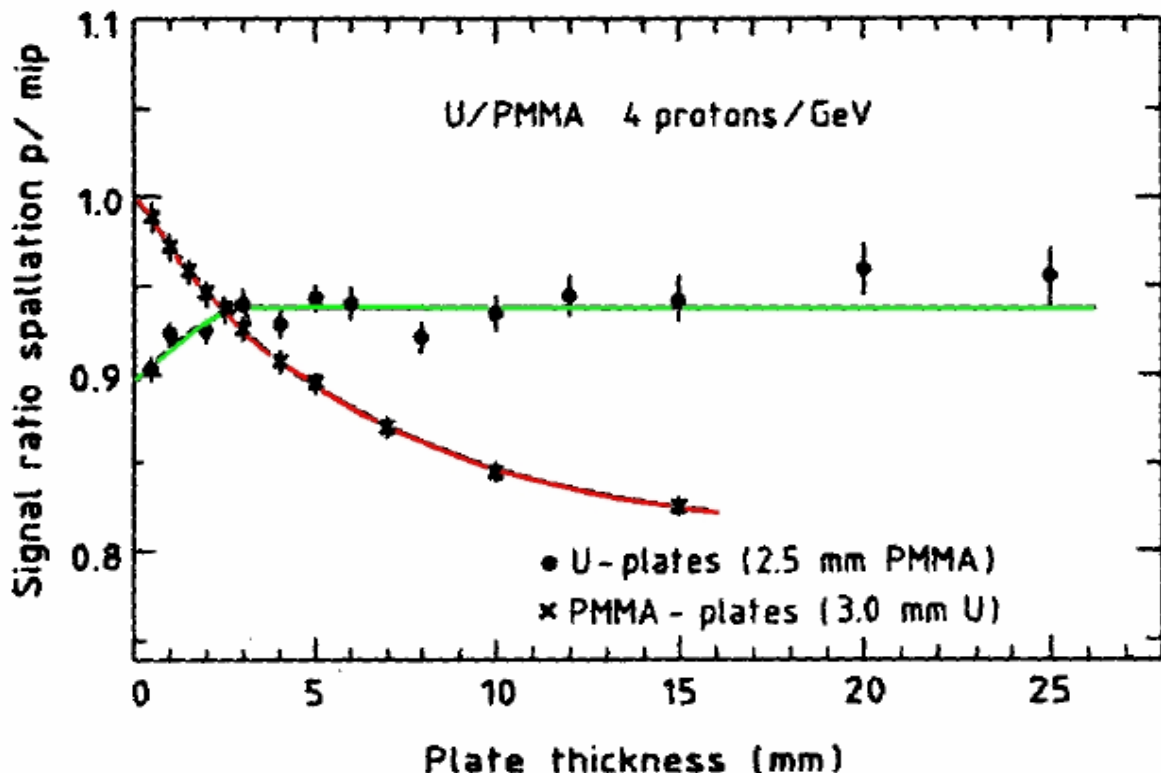
$\frac{ion}{mip} \nearrow$ if $d_{abs} \nearrow$

If $d_{abs} \gg R_{Proton}$

\rightsquigarrow only protons of surface region contribute

\rightsquigarrow saturation expected

Simulation:



Hardware Compensation: ZEUS

- $\frac{n}{mip}$

Neutrons have to be detected in active medium
Since energy transfer

$$\Delta E \sim \frac{E_n}{M_{act}}$$

Low mass media necessary (Birks !)

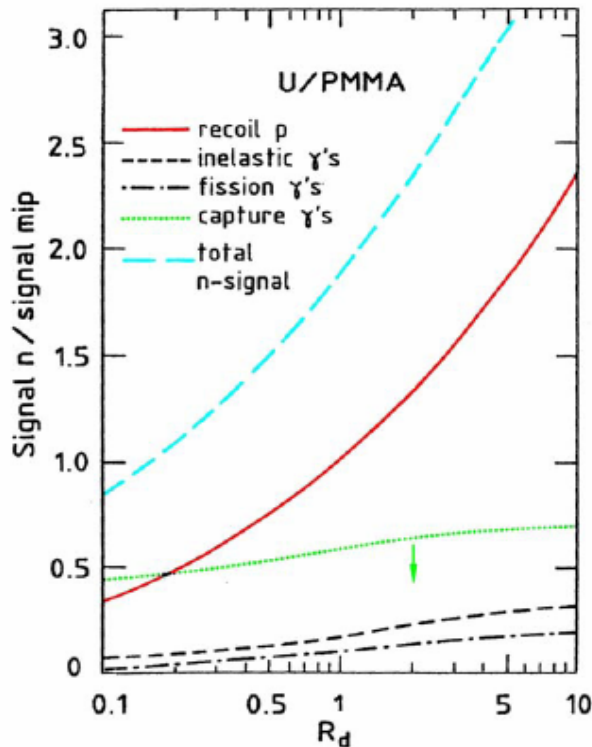
Scintillator optimal detection material

$$\frac{n}{mip} \nearrow \text{ if } \frac{d_{act}}{d_{pas}} = R_d^{-1} \searrow$$

since n are only stopped in active medium \rightsquigarrow
independent of d_{pas} , while

$$mip \nearrow \text{ if } \frac{d_{act}}{d_{pas}} \nearrow$$

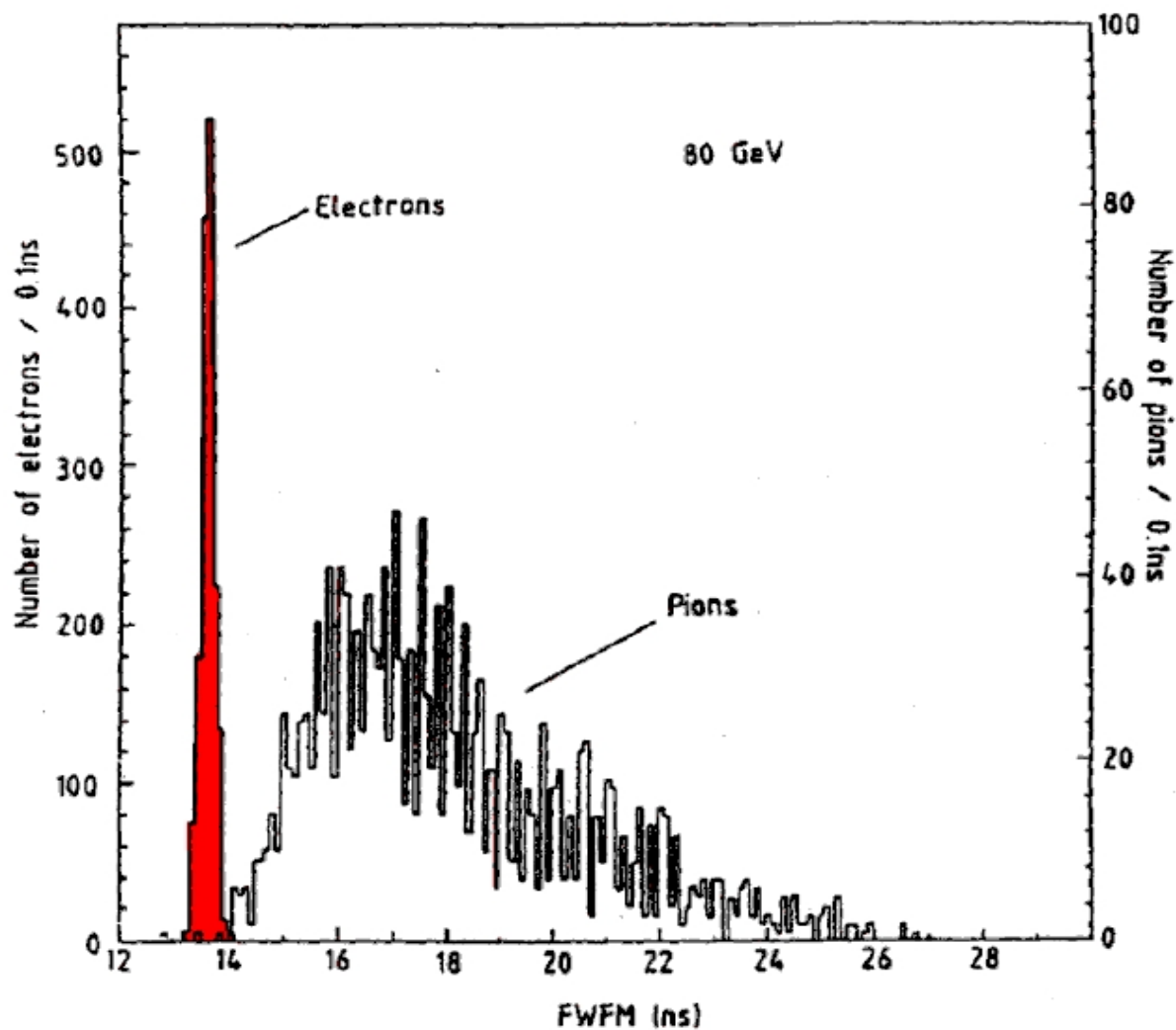
Monte Carlo simulation:



Hardware Compensation: ZEUS

Time dependence of signal complicated :

recoil protons "prompt" signal
capture gammas "delayed" signal



Hardware Compensation: ZEUS

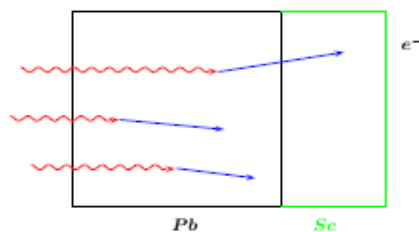
- $\frac{e}{mip}$

Instead of increasing $\frac{h_i}{mip}$ one can also decrease

$\frac{e}{mip}$ to achieve

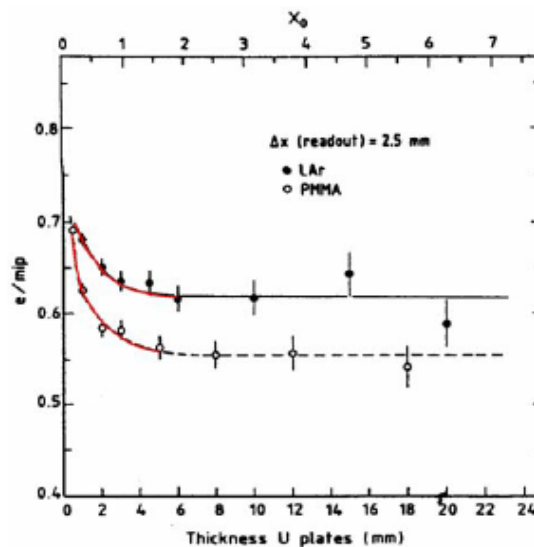
$$\frac{e}{mip} = \frac{h_i}{mip}$$

$\frac{e}{mip}$ decreases, if d_{abs} increases



$$\mu_{abs} \sim Z^4$$

Photons deposit energy dominantly in converter,
low energy electrons \rightsquigarrow small range \rightsquigarrow only
contribution from absorber surface region

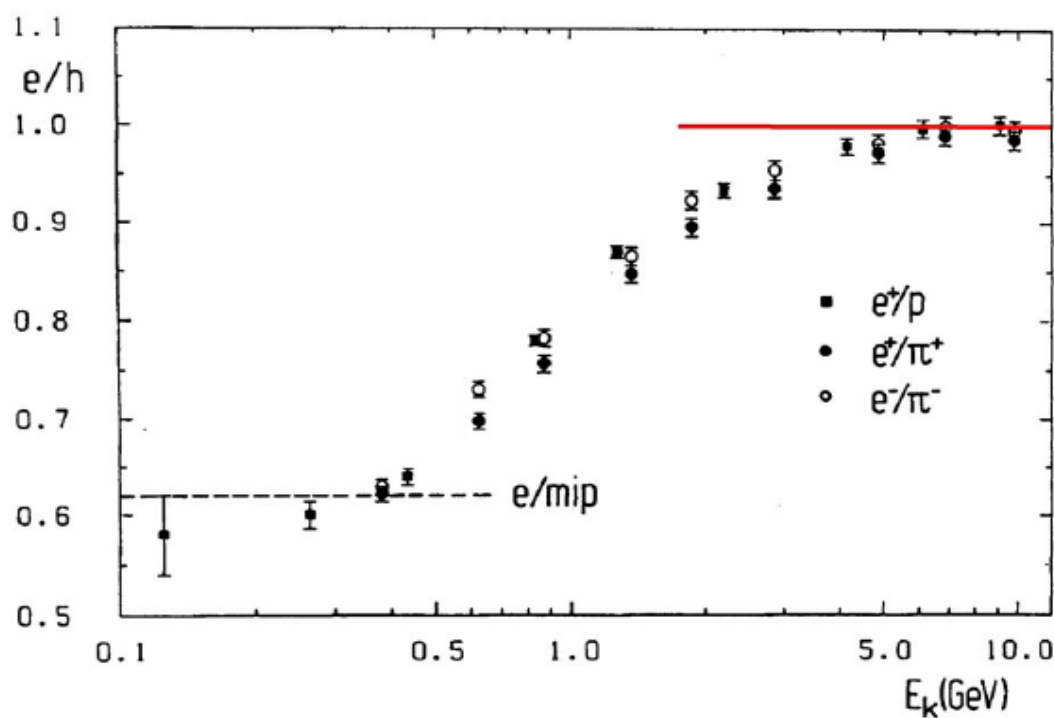
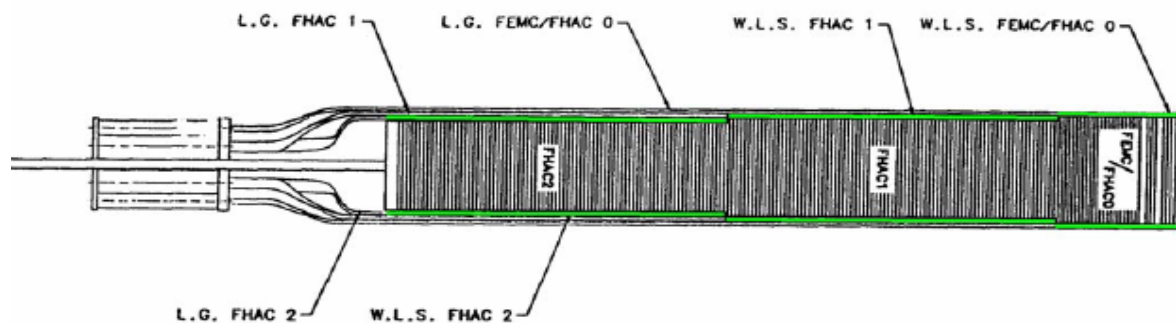


ZEUS: achieved compensation for
Pb–Sc–Calorimeter

linearity $\frac{\sigma}{E} = \frac{0.442 \text{ GeV}^{1/2}}{\sqrt{E}}$

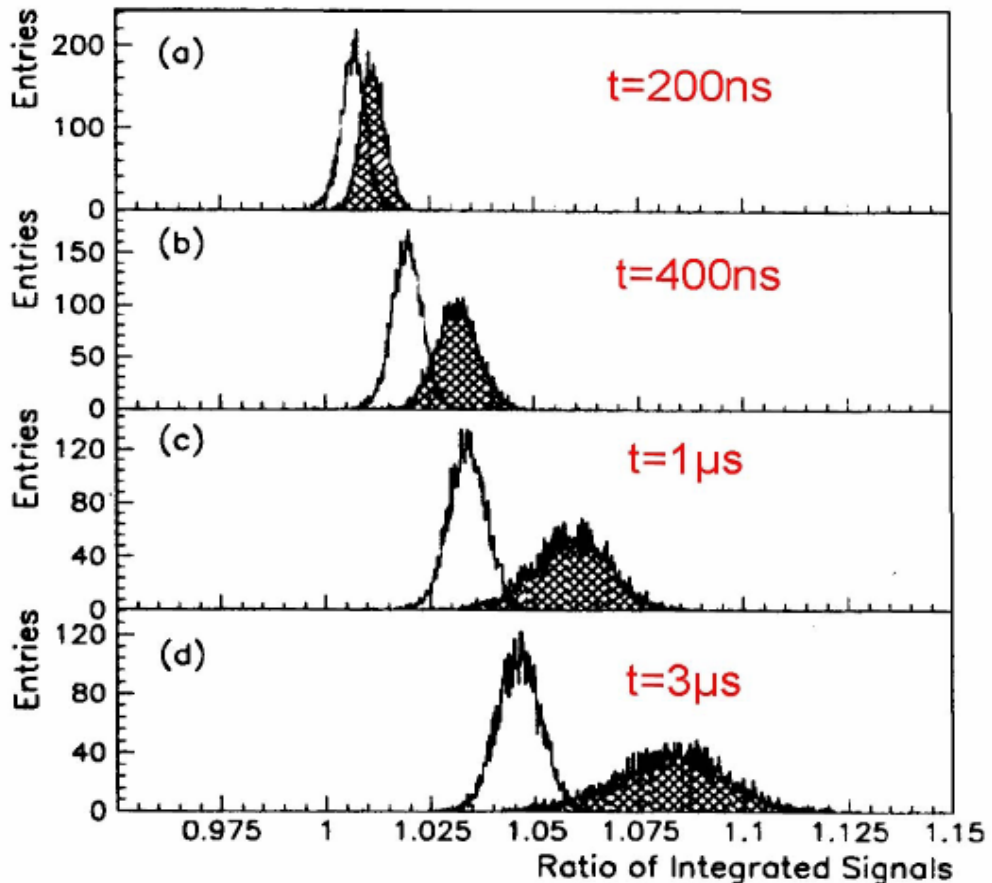
Hadron Calorimeter Systems: ZEUS

- Scintillator–U Compensating Calorimeter ZEUS
Module

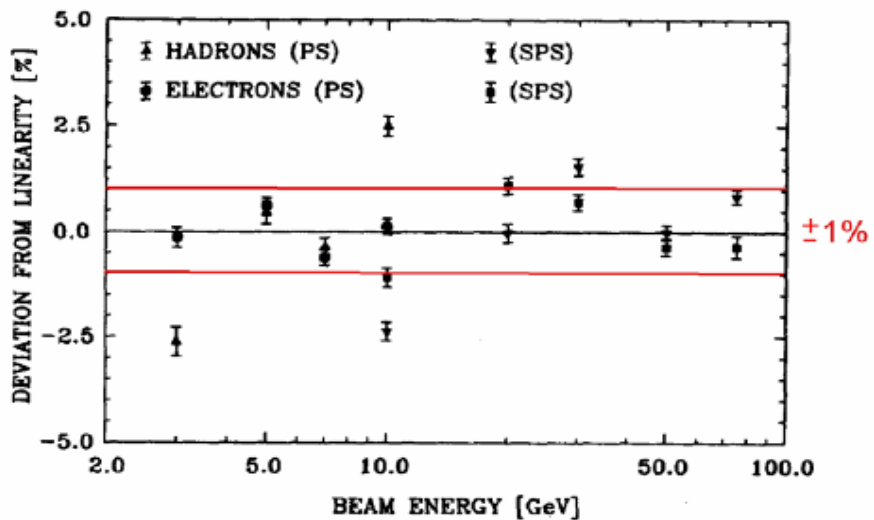


Hadron Calorimeter Systems: ZEUS

n-Contribution delayed

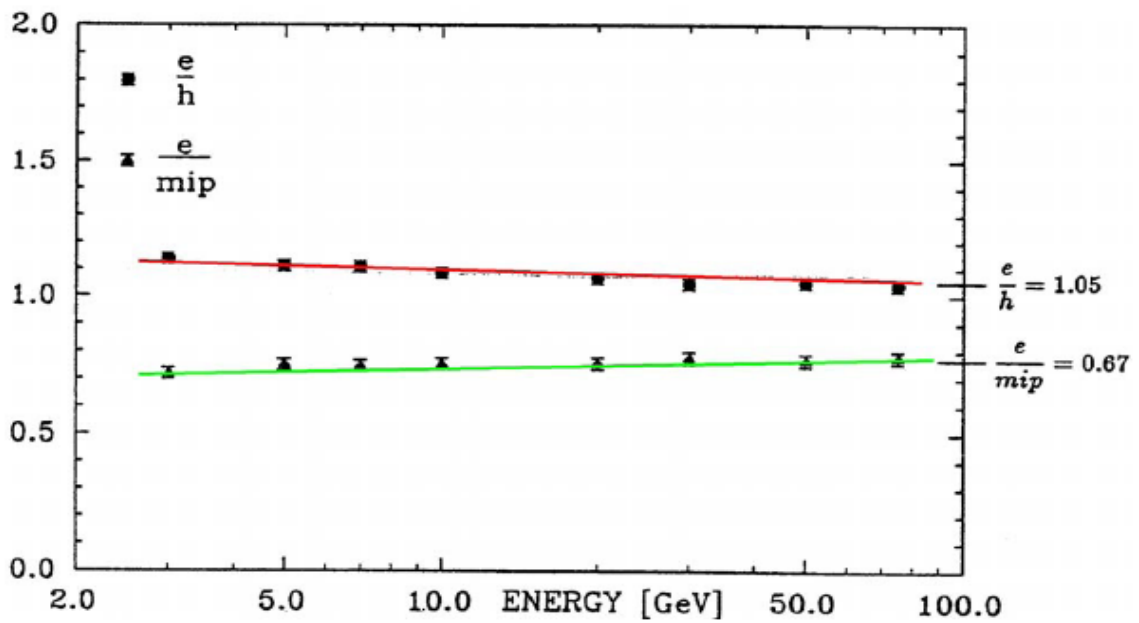
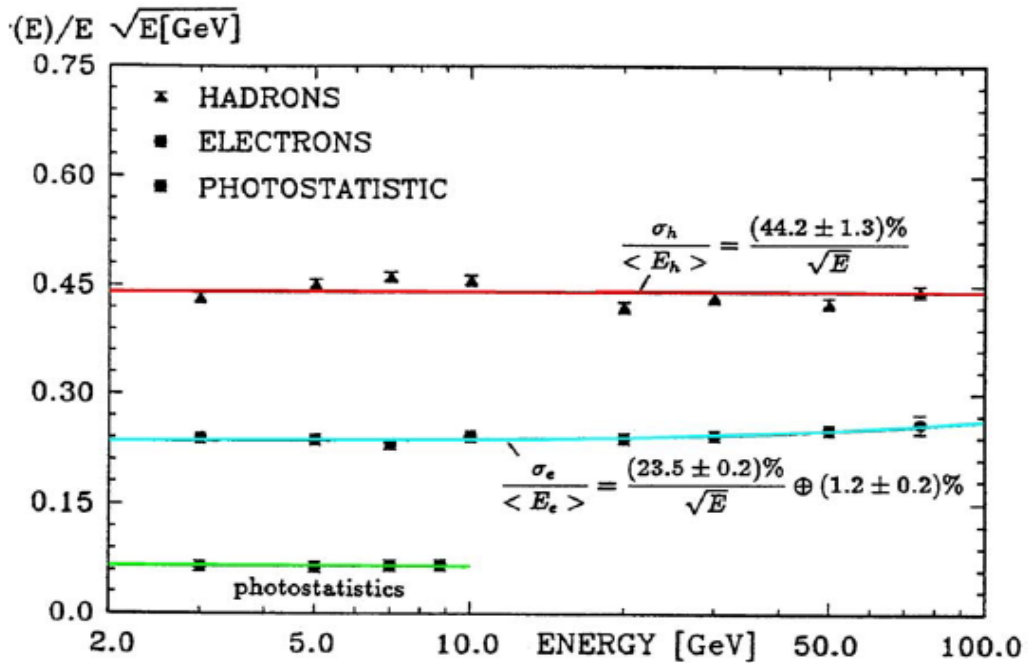


Linearity



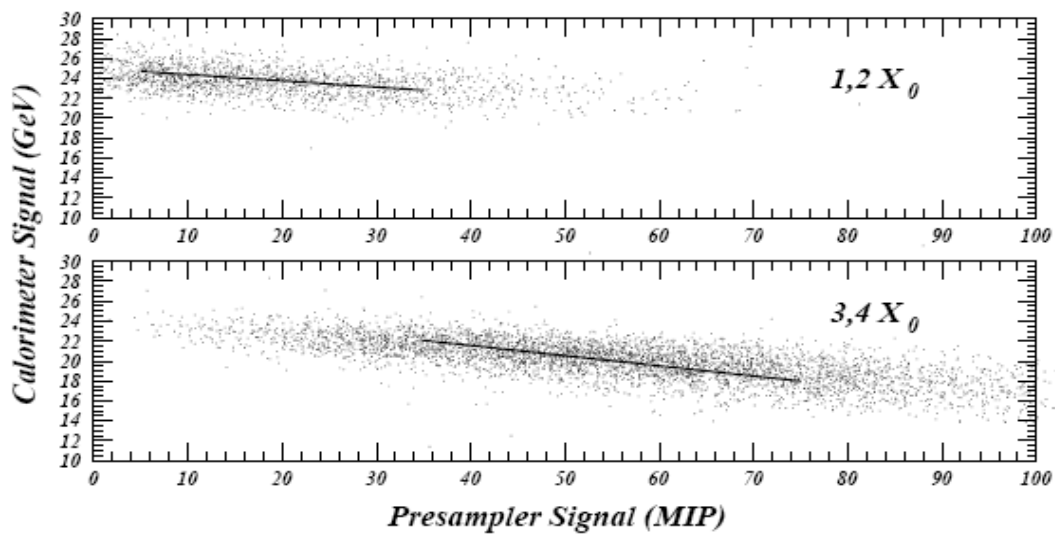
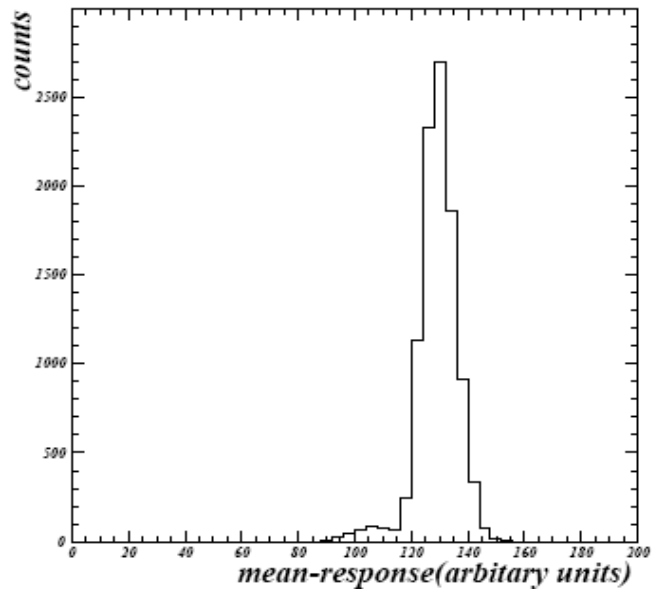
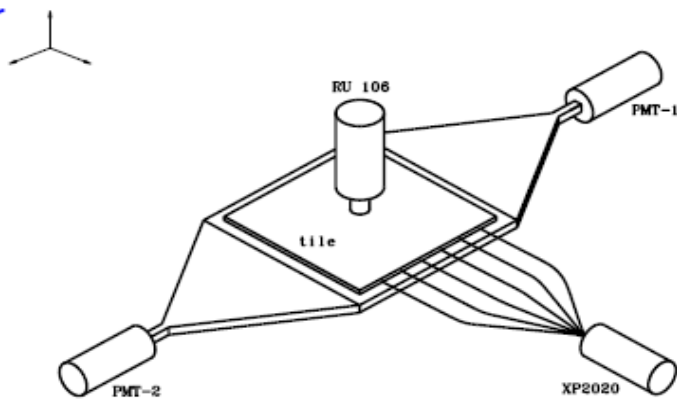
Hadron Calorimeter Systems: ZEUS

Resolution



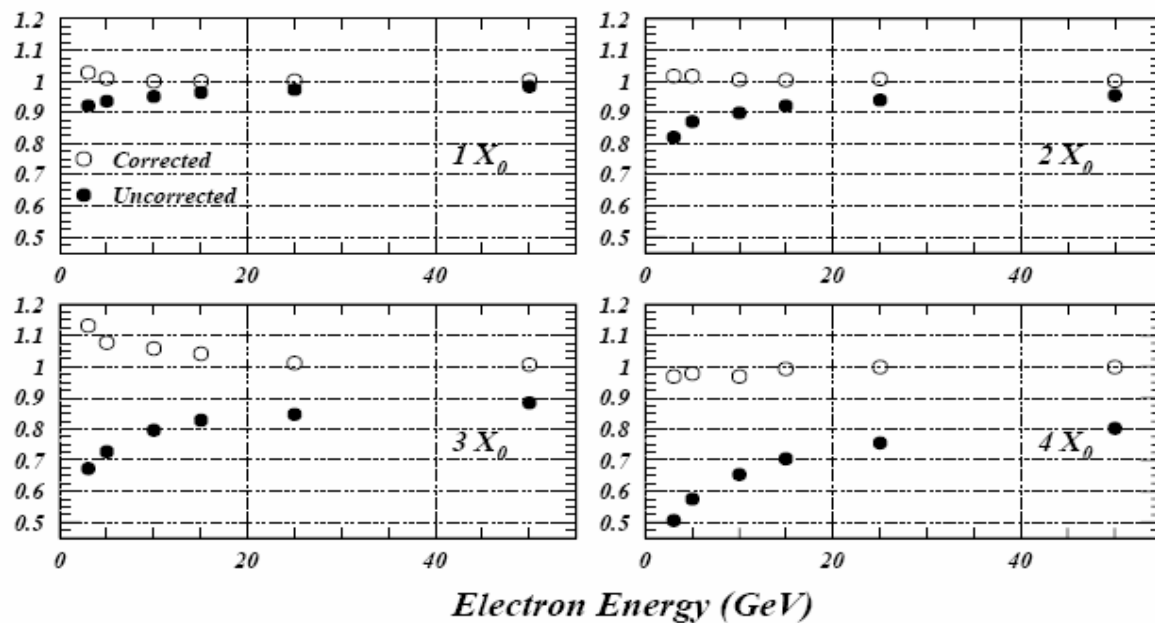
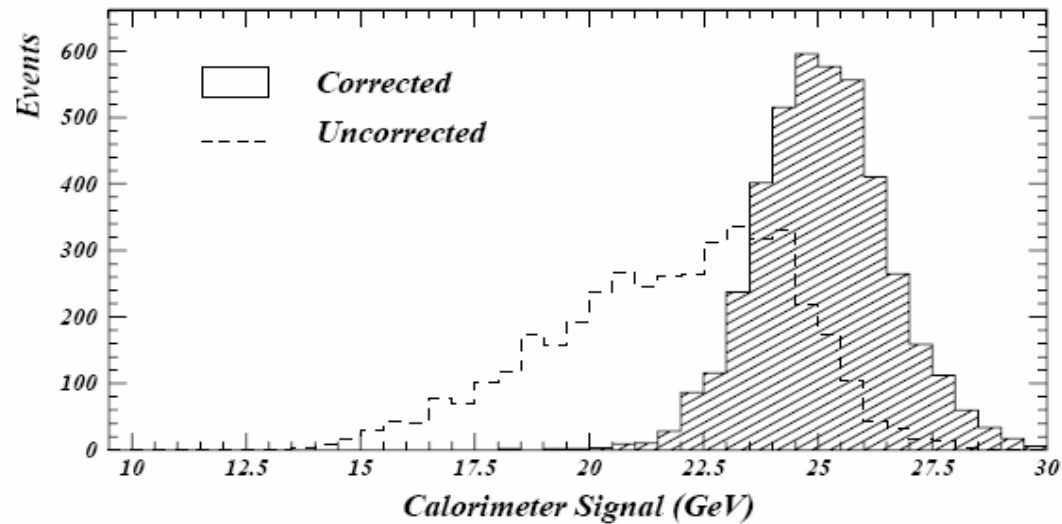
Hadron Calorimeter Systems: ZEUS

Presampler



Hadron Calorimeter Systems: ZEUS

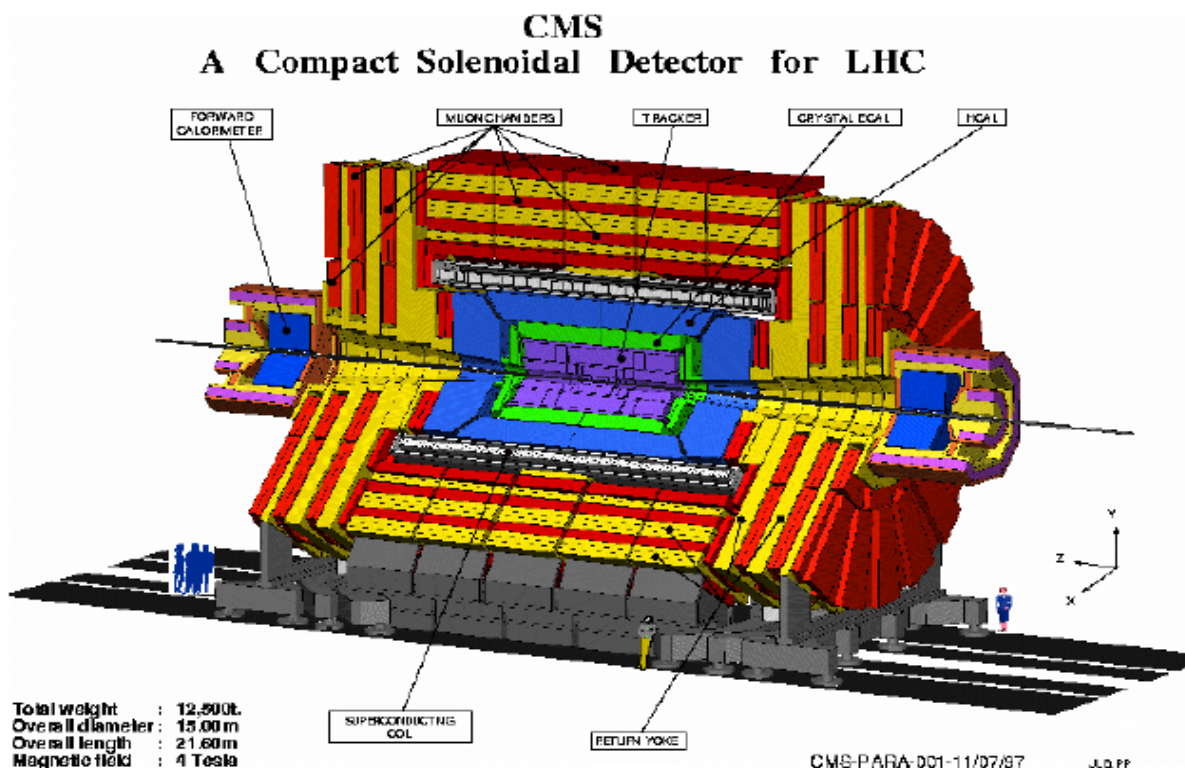
Achieve **Gaussian** shape



Further Optimization : Presampler
Hadron Electron Separator

Hadron Calorimeter Systems: CMS

Electromagnetic $PbWO_4$
Hadronic tile–calorimeter ($Sc + Cu$)



Technique: Calorimeter **inside coil**

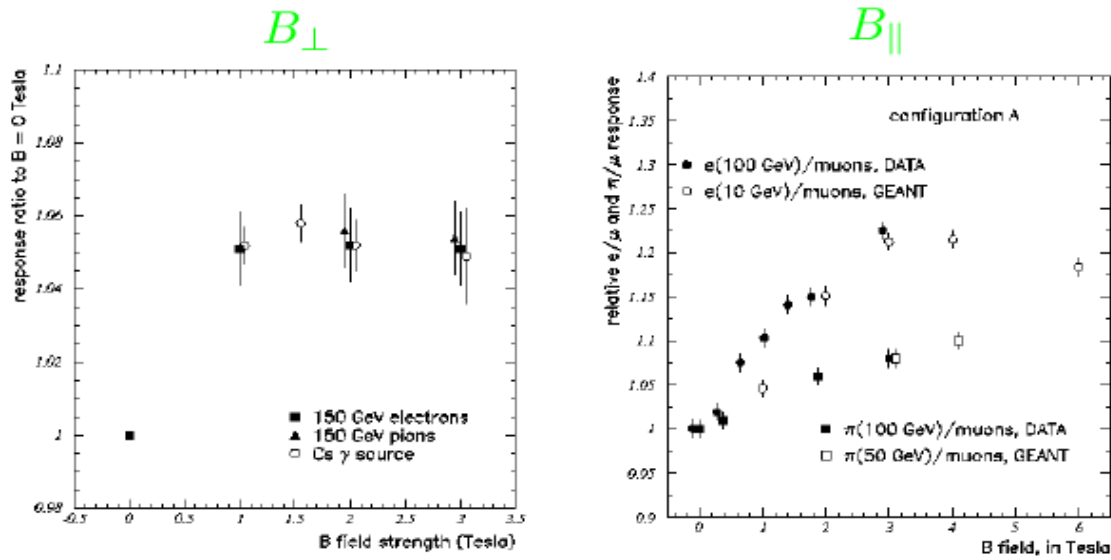
$PbWO_4$: electromagnetic

Scintillator – **Tile** calorimeter: hadronic

Hadron Calorimeter Systems: CMS

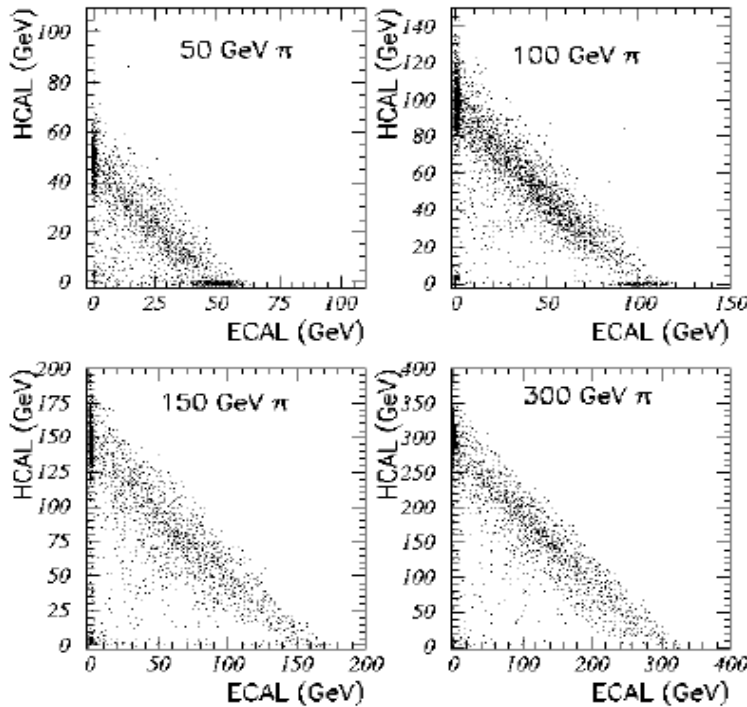
Results

- Dependence on B -field



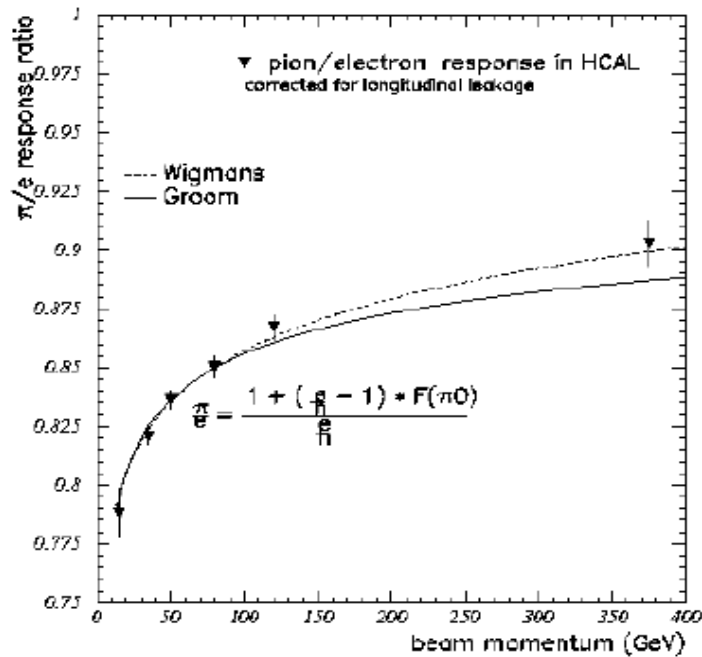
Explanation: B_{\perp} 3S to 1S mixing

- Energy sharing between ECAL and HCAL:

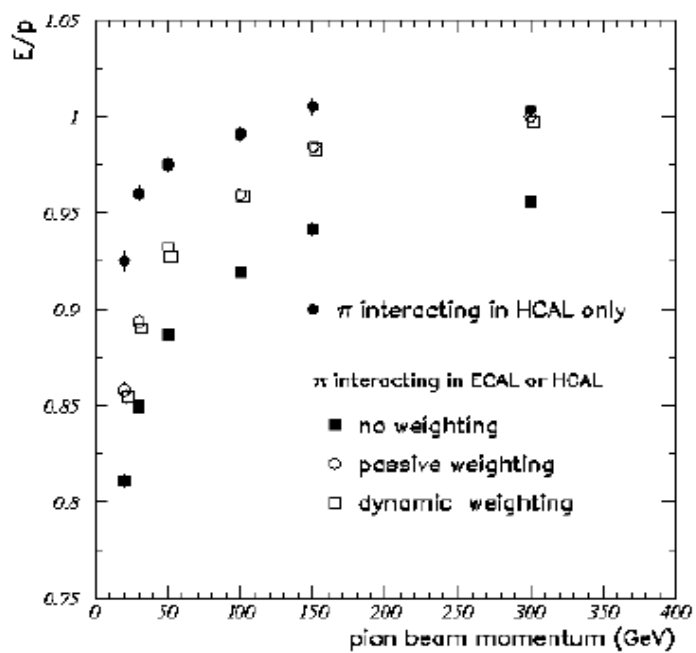


Hadron Calorimeter Systems: CMS

- $\frac{e}{\pi} \neq 1$

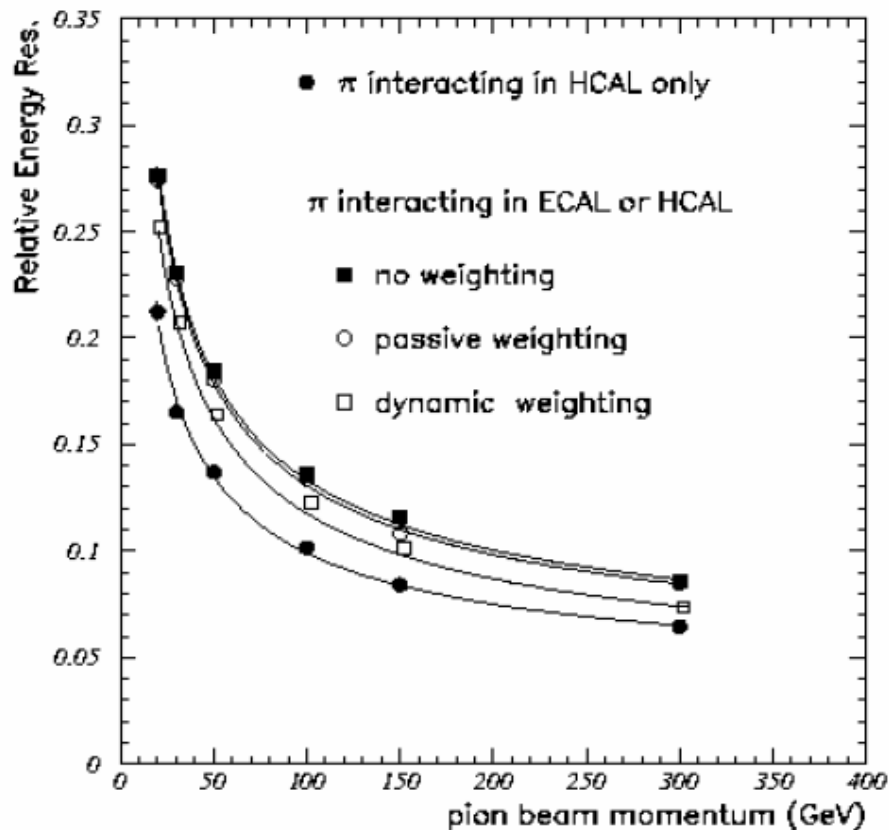


- Nonlinearity



Hadron Calorimeter Systems: CMS

- Resolution



Remark :

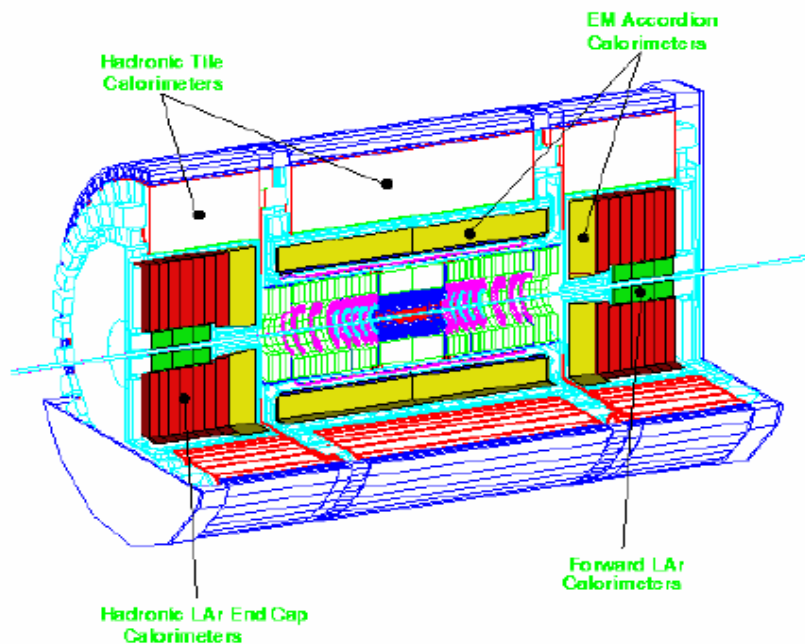
- Excellent energy resolution
for γ, e^- : $H \rightarrow \gamma\gamma$
- Poor hadron energy measurement

$$\left(\frac{\sigma}{E}\right)_{tile} = \frac{100\%}{\sqrt{E}} \oplus 4\%$$

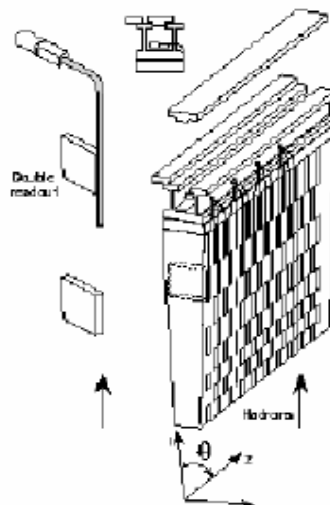
$$\left(\frac{\sigma}{E}\right)_{all} = \frac{127\%}{\sqrt{E}} \oplus 6.5\%$$

Hadron Calorimeter Systems: ATLAS

Detektor



Tile–calorimeter: hadron detection

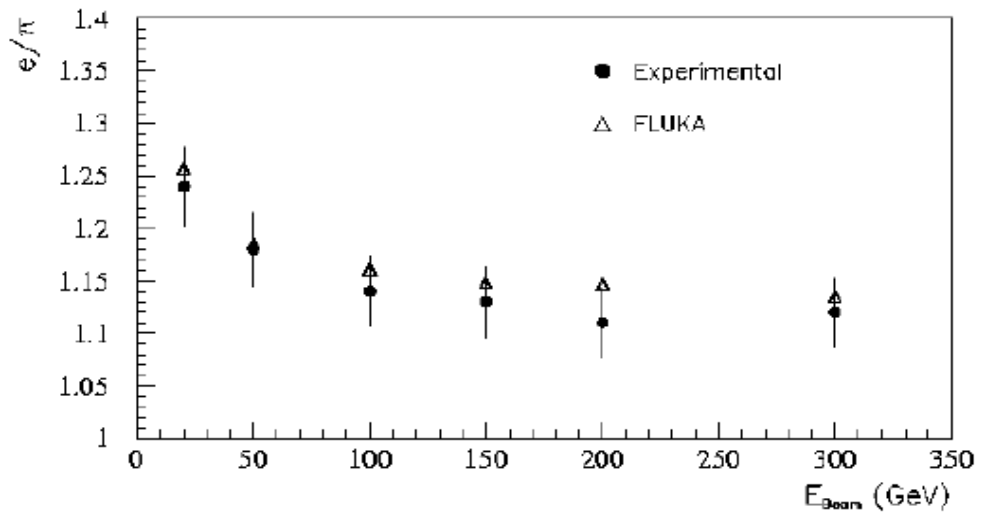


Hadrons

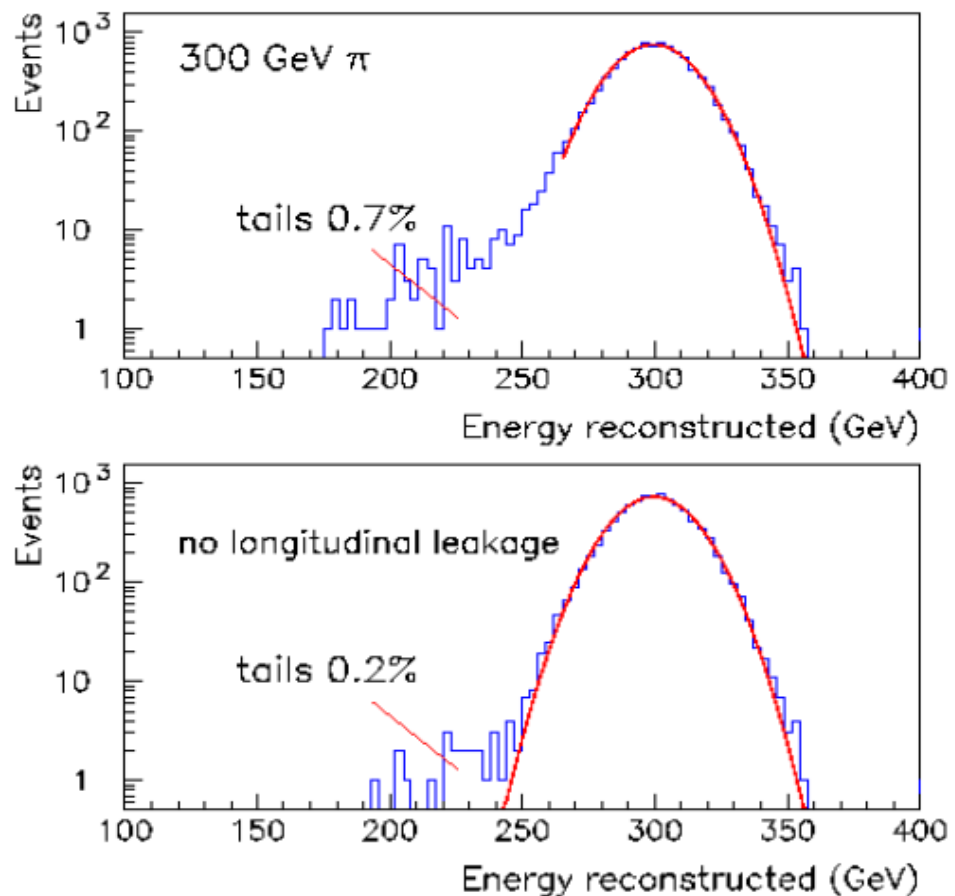
e/π -ratio :

$$\frac{e}{\pi} = \frac{\frac{e}{h}}{1 + (\frac{e}{h} - 1)0.11 \ln E}, \quad \frac{e}{h} = 1.37$$

Hadron Calorimeter Systems: ATLAS

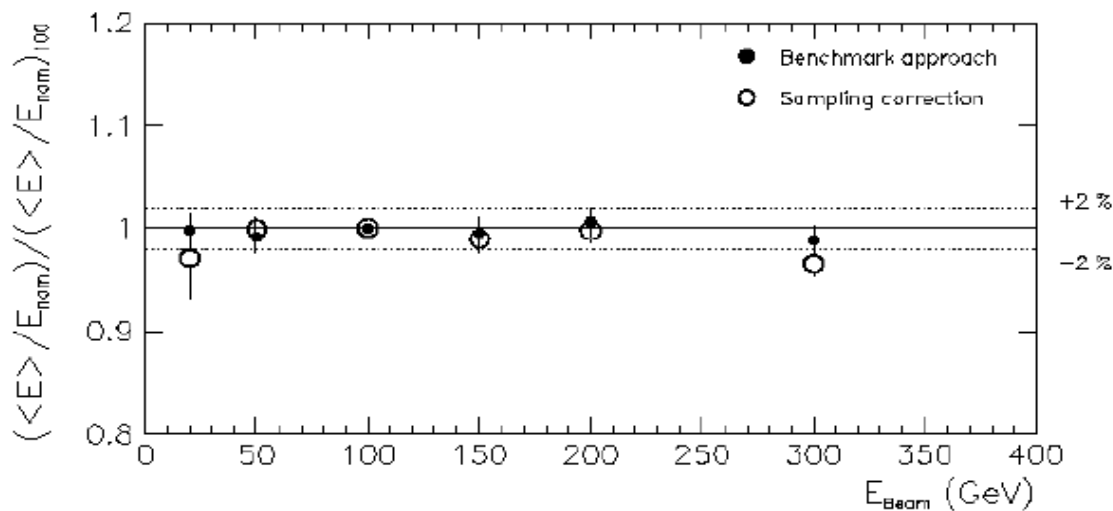


Gaussian–shape of signal

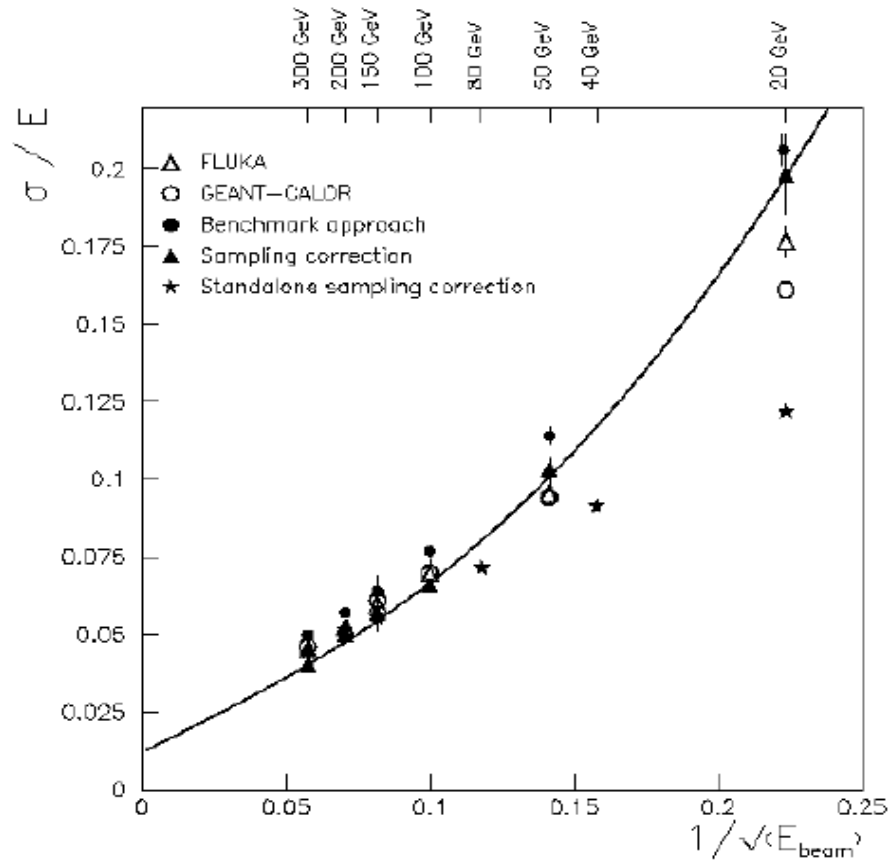


Hadron Calorimeter Systems: ATLAS

Linearity



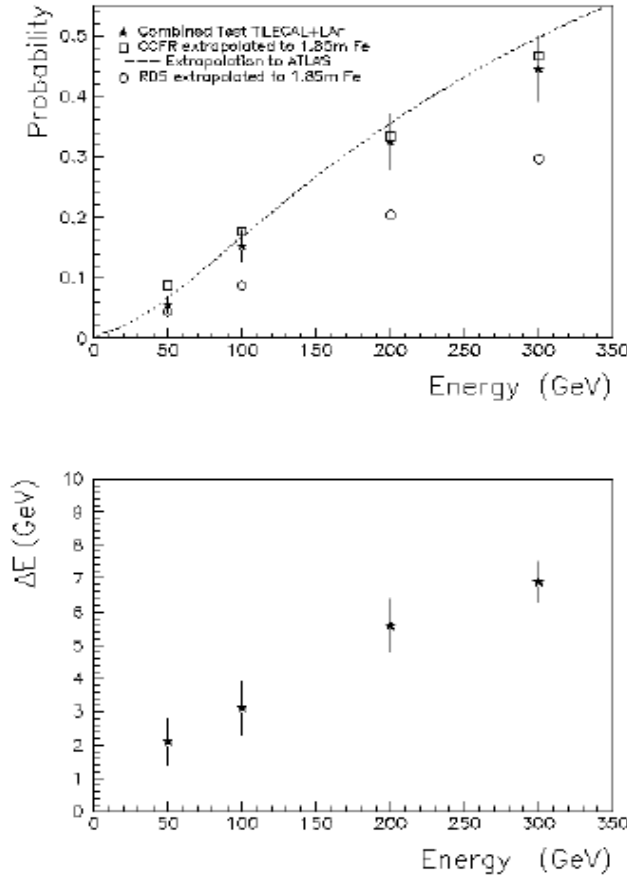
Energy resolution



Hadron Calorimeter Systems: ATLAS

Punch through

Probability large at 300 GeV:



Comparison: LHC-detectors

	ATLAS	CMS
$(\frac{\sigma}{E})_{em}$	$\frac{10\%}{\sqrt{E}} \oplus 0.35\%$	$\frac{4\%}{\sqrt{E}} \oplus 0.45\%$
$(\frac{\sigma}{E})_{had}$	$\frac{42\%}{\sqrt{E}} \oplus 1.8\%$	$\frac{127\%}{\sqrt{E}} \oplus 6.5\%$
$\sigma_\varphi \text{ had}$	$\frac{68 \text{ mrad}}{\sqrt{E}} \oplus 0.91 \text{ mrad}$	

Good/excellent electromagnetic calorimetry

$$H \rightarrow \gamma\gamma$$